
Stability of Manifold Neural Networks to Deformations

Zhiyang Wang

Dept. of Electrical and System Engineering
University of Pennsylvania
Philadelphia, PA 19104
zhiyangw@seas.upenn.edu

Luana Ruiz

Dept. of Electrical and System Engineering
University of Pennsylvania
Philadelphia, PA 19104
rbruiz@seas.upenn.edu

Alejandro Ribeiro

Dept. of Electrical and System Engineering
University of Pennsylvania
Philadelphia, PA 19104
aribeiro@seas.upenn.edu

Abstract

Stability is an important property of graph neural networks (GNNs) which explains their success in many problems of practical interest. Existing GNN stability results depend on the size of the graph, restricting applicability to graphs of moderate size. To understand the stability properties of GNNs on large graphs, we consider neural networks supported on manifolds. These are defined in terms of manifold diffusions mediated by the Laplace-Beltrami (LB) operator and are interpreted as limits of GNNs running on graphs of growing size. We define manifold deformations and show that they lead to perturbations of the manifold’s LB operator that consist of an absolute and a relative perturbation term. We then define filters that split the infinite dimensional spectrum of the LB operator in finite partitions, and prove that manifold neural networks (MNNs) with these filters are stable to both, absolute and relative perturbations of the LB operator. Stability results are illustrated numerically in resource allocation problems in wireless networks.

1 Introduction

Inspired by convolutional neural networks (CNNs), graph neural networks (GNNs) are made up of layers consisting of banks of graph convolutional filters composed with pointwise nonlinearities [16, 6, 23]. A growing body of work has demonstrated the success of GNNs in tasks as diverse as learning ratings in recommendation systems [5, 22] and learning resource allocations in wireless communication networks [4, 21]. Recent theoretical work has demonstrated that the good performance of GNNs is explained by invariance and stability properties they inherit from convolutions [15]. This is akin to seminal work proving that the same is true of CNNs [11]. Where CNNs can be shown to be equivariant to translation and stable to deformations of Euclidean space [11], GNNs can be shown to be equivariant to permutations and stable to deformations of the graph [8, 24].

Existing stability analyses of GNNs yield bounds that grow with the number of nodes in the graph [8, 24]. This is not only an important limitation but one that runs counter to empirical and theoretical evidence: GNNs are known to work well for large graphs and we can think of Euclidean space as a dense limit of a discretization graph. Our goal in this paper is to fill this gap by studying stability properties of manifold neural networks (MNNs). A manifold is a geometric object with possibly

irregular structure. Thus, discretizations of a manifold yield models for possibly irregular graphs of arbitrarily large size with well defined limits [2, 3, 10]. In studying stability of MNNs, we derive results that hold for such limit objects and therefore illustrate the stability of GNNs for graphs representing discretizations of the manifold with arbitrarily many nodes.

To study stability properties of MNNs, we start by showing that manifold deformations lead to absolute and relative perturbations of the manifold’s Laplace-Beltrami (LB) operator (Theorem 2). We then analyze the stability of MNNs to absolute (Section 3.1) and relative (Section 3.2) LB perturbations. Since perturbations of the LB operator perturb its spectrum, we introduce two types of spectral manifold filters, the frequency difference threshold (FDT) filter (Definition 3) and the frequency ratio threshold (FRT) filter (Definition 7). These filters, which can be implemented as convolutions, mitigate the spectral effects of absolute and relative eigenvalue perturbations respectively, grouping eigenvalues that are less than a certain threshold apart to make sure that they have similar frequency responses. Using FDT and FRT filters satisfying certain Lipschitz continuity assumptions, we can build MNNs that are stable to manifold deformations as stated in the following theorem.

Theorem 1 (MNN stability to deformations). Let $\Phi(f)$ be a MNN with fixed parameters on the manifold \mathcal{M} and assume that the convolutional filters of this MNN are FDT, FRT, Lipschitz and integral Lipschitz. Suppose that \mathcal{M} undergoes a deformation $v(x) = x + \tau(x) \in \mathcal{M}$ where $\|\tau(x)\| = \epsilon$ and $\|\nabla \tau(x)\| = \epsilon$. Then, under mild assumptions,

$$\|\Phi(f \circ v) - \Phi(f)\|^2 = O(\epsilon^2) \|f\|^2.$$

This is the main result of this paper, and it is a direct consequence of two results of independent interest that we prove in Sections 3.1 and 3.2: that MNNs with FDT filters satisfying a Lipschitz continuity assumption (Definition 4) are stable to absolute perturbations (Theorem 3); and that MNNs with FRT filters satisfying an integral Lipschitz continuity assumption (Definition 8) are stable to absolute perturbations (Theorem 4). A formal statement of Theorem 1 is available in the supplementary materials.

1.1 Related Work

The importance of stability to deformations in understanding the merits of generic convolutional neural networks relative to the respective convolutional filters, traces back to the seminal work on Euclidean scattering transforms [11]. This work inspired extensions of the analysis to graph scattering transforms [7, 24] and GNNs [8, 20, 24]. Common to all of these works is the introduction of domain (graph, or Euclidean) deformations and the proof of Lipschitz stability with respect to the norm of the deformation for some filter categories. The similar stability properties of CNNs and GNNs have been shown to be a consequence of their shared algebraic structure [12].

All of the GNN stability results described above have bounds that grow with the number of nodes in the graph. Overcoming this limitation has motivated the study of neural networks on graphons [14, 15, 9]. Results in this setting are independent of graph size – same as the results presented here, they hold for a limit object – but it must be pointed out that graphons are limits of dense graphs in the sense that they have growing degree. This is different from graphs sampled from manifolds that have constant as the discretization becomes finer [10]. Of particular relevance to our paper is work on GNN transferability for graphs that are sampled from a manifold [10]. This work shows that GNNs on a graph sampled from a manifold are close to the respective MNN. They can be combined with our stability results to prove stability of GNNs on graphs sampled from perturbed manifolds.

2 Preliminary Definitions

Before looking deeper into the stability of neural networks on manifolds, we first review the definition of Riemannian manifolds and information processing architectures — namely the convolutional filters and convolutional neural networks — for data supported on them.

2.1 Data on Manifolds

A differentiable d -dimensional manifold \mathcal{M} is a topological space where each point $x \in \mathcal{M}$ has a neighborhood that is homeomorphic to a d -dimensional Euclidean space. This is called a tangent

space which contains all the tangent vectors at this point. Generally speaking, a manifold is a space that is locally Euclidean, i.e., it is Euclidean around each point. A *Riemannian manifold* is a pair (\mathcal{M}, g) where \mathcal{M} is a real and smooth manifold, while g is a Riemannian metric that assigns to each point $x \in \mathcal{M}$ a positive-definite inner product $g_x : T_x \mathcal{M} \times T_x \mathcal{M} \rightarrow \mathbb{R}$, with $T_x \mathcal{M}$ the tangent space at point $x \in \mathcal{M}$. The disjoint union of all tangent spaces on (\mathcal{M}, g) is called the tangent bundle $T\mathcal{M}$. In this paper, we always assume manifolds to be Riemannian and represent them as \mathcal{M} for simplicity. We consider two types of functions defined on \mathcal{M} : scalar functions and tangent vector functions. The former maps each point on the manifold to some real value, while the latter attaches a tangent vector to each point. The L^2 spaces of these functions are denoted as $L^2(\mathcal{M})$ and $L^2(T\mathcal{M})$ respectively.

Data supported on \mathcal{M} can be represented as smooth scalar functions denoted as $f \in L^2(\mathcal{M}) : \mathcal{M} \rightarrow \mathbb{R}$. In other words, we define manifold data in a point-wise fashion by attaching value $f(x)$ to the datum at each point $x \in \mathcal{M}$. Our goal is to understand how to process manifold data. To do so, we need to figure out how it varies on the manifold, i.e., how to take derivatives of the function $f \in L^2(\mathcal{M})$. On manifolds, differentiation is generalized by using the local tangent space. The differential operator is the *intrinsic gradient* [13], defined as the operator $\nabla : L^2(\mathcal{M}) \rightarrow L^2(T\mathcal{M})$ which characterizes the direction of the fastest change of a function at a given point, with the direction indicated by a tangent vector in $L^2(T\mathcal{M})$. The adjoint of the intrinsic gradient is the *intrinsic divergence*, which is defined as $\text{div} : L^2(T\mathcal{M}) \rightarrow L^2(\mathcal{M})$, and measures the net flow of a tangent vector at a point.

The Laplace-Beltrami (LB) operator \mathcal{L} , which is a generalization of the Laplace operator to Riemannian manifolds, is defined by composing the intrinsic divergence and the intrinsic gradient. Formally,

$$\mathcal{L}f = -\text{div} \circ \nabla f = -\langle \nabla, \nabla \rangle f. \quad (1)$$

Analogous to the Laplace operator in Euclidean domains and the Laplacian matrix in the case of graphs, the LB operator provides a measure of a function's total variation, i.e., it describes how much the local average of the function values around a point deviates from the function value at this point itself [2]. In the following, unless otherwise specified, the gradient and LB operators are carried out locally around x in the tangent space $T_x \mathcal{M}$, i.e., $\mathcal{L} = \mathcal{L}_x$ and $\nabla = \nabla_x$.

We focus on compact Riemannian manifolds such that the LB operator is self-adjoint and positive-semidefinite. Thus, the operator \mathcal{L} possesses a discrete spectrum $\{\lambda_i, \phi_i\}_{i \in \mathbb{N}^+}$ with real eigenvalues λ_i and corresponding eigenfunctions ϕ_i . This allows it to be written as $\mathcal{L}\phi_i = \lambda_i\phi_i$, $i = 1, 2, \dots$. The eigenvalues are positive and ordered in increasing order as $0 < \lambda_1 \leq \lambda_2 \leq \lambda_3 \leq \dots$ while the eigenfunctions are orthonormal. For a manifold of d dimensions, λ_i is known to grow in the order of $i^{2/d}$ as a consequence of Weyl's law [1].

Due to orthonormality, the eigenfunctions of the LB operator can be seen as a generalized eigenbasis in an intrinsic sense. This allows interpreting the ϕ_i as oscillation modes and the λ_i as corresponding oscillation "frequencies". A square-integrable function $f \in L^2(\mathcal{M})$ can be represented in this eigenbasis as

$$f = \sum_{i=1}^{\infty} \langle f, \phi_i \rangle \phi_i. \quad (2)$$

This spectral representation of f allows us to rewrite (1) as

$$\mathcal{L}f = \sum_{i=1}^{\infty} \lambda_i \langle f, \phi_i \rangle \phi_i. \quad (3)$$

2.2 Manifold Convolutions

On manifolds, the notion of diffusion arises from the solution of the wave equation,

$$\frac{\partial^2 f(x, t)}{\partial t^2} = \mathcal{L}f(x, t) \quad (4)$$

where $f(x, t)$ denotes manifold data f at time t and \mathcal{L} is the LB operator defined in (1). With an initial condition $f(x, 0) = f(x)$, the solution of this equation is given by

$$f(x, t) = e^{-\sqrt{\mathcal{L}}t} f(x) \quad (5)$$

where we interpret $e^{-\sqrt{\mathcal{L}}}$ as an instantaneous diffusion or shift.

Given a function $h(t)$, (5) allows writing the continuous-time convolution of h and f as

$$\int_0^\infty h(t)f(x, t)dt = \int_0^\infty h(t)e^{-\sqrt{\mathcal{L}}t}f(x)dt. \quad (6)$$

Since in this paper we consider a finite and discrete time scale, letting $h_k = h(k)$ for $0 \leq k \leq K-1$ denote K filter coefficients we define the discrete-time manifold convolution as

$$\mathbf{h}(\mathcal{L})f := \sum_{i=1}^{\infty} \sum_{k=0}^{K-1} h_k e^{-\sqrt{\lambda_i}k} \langle f, \phi_i \rangle \phi_i \quad (7)$$

where we have used (2) to substitute $e^{-\sqrt{\mathcal{L}}t}$. This convolution admits a spectral representation or frequency response

$$h(\lambda) = \sum_{k=0}^{K-1} h_k e^{-\sqrt{\lambda}k} \quad (8)$$

obtained by projecting $\mathbf{h}(\mathcal{L})$ onto the eigenfunctions $\{\phi_i\}_{i \in \mathbb{N}^+}$. The frequency response $h(\lambda)$ only depends on the filter coefficients and the eigenvalues of \mathcal{L} .

Note that, by taking the first-order Taylor expansion of the exponential, the frequency response in (8) could be approximated by a polynomial. The manifold convolution $\mathbf{h}(\mathcal{L})$ (7) can thus realize any smooth spectral response $h(\lambda)$ with convergent Taylor series around the λ_i as $K \rightarrow \infty$ [19]. Hence, for a generic function h satisfying these conditions, we may also write the manifold convolution (7) as

$$\mathbf{h}(\mathcal{L})f := \sum_{i=1}^{\infty} h(\lambda_i) \langle f, \phi_i \rangle \phi_i. \quad (9)$$

2.3 Manifold Neural Networks

Manifold neural networks (MNNs) are deep convolutional architectures consisting of L layers where each layer implements two operations: a convolutional filterbank and a pointwise nonlinearity. At each layer $l = 1, 2, \dots, L$, the convolutional filters map the incoming F_{l-1} features from layer $l-1$ into F_l features which are then processed by a nonlinearity σ . Explicitly,

$$f_l^p(x) = \sigma \left(\sum_{q=1}^{F_{l-1}} \mathbf{h}_l^{pq}(\mathcal{L}) f_{l-1}^q(x) \right), \quad (10)$$

where $\mathbf{h}_l^{pq}(\mathcal{L})$ is the filter mapping the q -th feature from layer $l-1$ to the p -th feature of layer l for $1 \leq q \leq F_{l-1}$ and $1 \leq p \leq F_l$ as (9) shows. At the first layer, the input features are the input data f^q for $1 \leq q \leq F_0$. The output features of the MNN are the ones produced by the L -th layer, which are given by $y^p = f_L^p$ for $1 \leq p \leq F_L$.

To represent the MNN more succinctly, we may gather the coefficients of the manifold convolutional filters \mathbf{h}_l^{pq} across all layers in a tensor \mathbf{H} , and define the MNN map $\mathbf{y} = \Phi(\mathbf{H}, \mathcal{L}, f)$. This map emphasizes that the MNN is parameterized by both the filter functions and the LB operator \mathcal{L} .

3 Stability of Manifold Neural Networks

On the manifold \mathcal{M} , we define a deformation $v : \mathcal{M} \rightarrow \mathcal{M}$ as $v(x) = x + \tau(x)$, where $x \in \mathcal{M}$ is a point on the manifold and $\tau(x)$ represents a small displacement in the neighborhood of x . Typically, $\|\tau(x)\|$ and $\|\nabla \tau(x)\|$ are upper bounded. Their bounds can be used to characterize the size of the deformation. Let $f : \mathcal{M} \rightarrow \mathbb{R}$ represent data supported on the manifold. Because \mathcal{M} is the codomain of v , $g = f \circ v$ maps points $v(x) \in \mathcal{M}$ to $f(v(x)) \in \mathbb{R}$ and so it is still a scalar function on \mathcal{M} . Hence, we can think of the effect of a deformation on manifold data as a perturbation of functions f into functions g supported on the same manifold.

Applying the LB operator of \mathcal{M} to function g , we can get $p = \mathcal{L}g$. Since p is also a function on \mathcal{M} , we may define the operator \mathcal{L}' mapping f directly into p as

$$p(x) = \mathcal{L}'f(x) = \mathcal{L}g(x) = \mathcal{L}f(v(x)) = -\langle \nabla, \nabla \rangle f(v(x)). \quad (11)$$

We refer to \mathcal{L}' as the perturbed LB operator, i.e., the operator resulting from the deformation v . Under the assumption that the manifold is smooth (Assumption 1), the difference between \mathcal{L}' and \mathcal{L} is stated in the following theorem and proved in the supplementary material.

Assumption 1 (Smoothness of the manifold). The gradient operator ∇ of manifold \mathcal{M} satisfies $\|\nabla_y - \nabla_x\| \leq \|y - x\|$ and $\|\nabla\| \leq 1$.

Theorem 2. Let \mathcal{L} be the LB operator of manifold \mathcal{M} . Consider a deformation $v(x) = x + \tau(x) \in \mathcal{M}$ to points on \mathcal{M} with $\|\tau(x)\| = \epsilon$ and $\|\nabla\tau(x)\| = \epsilon$. Under Assumption 1, the difference between the original operator and the deformed operator can be written as

$$\mathcal{L} - \mathcal{L}' = \mathbf{E}\mathcal{L} + \mathbf{A}, \quad (12)$$

for some operators \mathbf{E} and \mathbf{A} with norms $\|\mathbf{E}\| = O(\epsilon)$ and $\|\mathbf{A}\| = O(\epsilon)$.

In conclusion, the difference between the original LB operator and the LB operator of the perturbed manifold can be represented by a combination of an absolute perturbation \mathbf{A} [cf. Definition 1] and a relative perturbation $\mathbf{E}\mathcal{L}$ [cf. Definition 5]. We thus study the stability of MNNs under deformations of the manifold by considering absolute and relative LB perturbations respectively.

3.1 Stability to Absolute Perturbations of \mathcal{L}

We start by analyzing the stability of MNNs to absolute perturbations to the LB operator, which are generic additive perturbations defined as follows.

Definition 1 (Absolute perturbations). Let \mathcal{L} be the LB operator of manifold \mathcal{M} . An absolute perturbation of \mathcal{L} is defined as

$$\mathcal{L}' - \mathcal{L} = \mathbf{A}, \quad (13)$$

where \mathbf{A} , called the absolute perturbation operator, is symmetric.

Like \mathcal{L} , the operator \mathcal{L}' resulting from an absolute perturbation is self-adjoint due to the symmetry of \mathbf{A} . Hence, it can be decomposed into its eigenvalues and eigenfunctions as (1) shows. Based on the formulation of the MNNs that we have established in (10), the manifold convolutional filters defined in (9) only rely on the evaluation of $h(\lambda)$ at each λ_i when the filter coefficients are fixed. To understand the effect of absolute perturbations on the filters that make up the layers of a MNN, it thus suffices to look at how the eigenvalues are perturbed. The challenge in this case is that the spectrum of \mathcal{L} on a manifold is infinite-dimensional, which leads to an infinite (though countable) number of eigenvalue perturbations that need to be taken into account. Fortunately, as demonstrated by Proposition 1 large eigenvalues accumulate in certain parts of the real line, suggesting a strategy to partition the spectrum into a finite number of groups.

Proposition 1. Consider a d -dimensional manifold \mathcal{M} and let \mathcal{L} be its LB operator with eigenvalues $\{\lambda_k\}_{k=1}^\infty$. Let C_1 denote an arbitrary constant and let C_d be the volume of the d -dimensional unit ball. For any $\alpha > 0$ and $d > 2$, there exists N_1 given by

$$N_1 = \lceil (ad/C_1)^{d/(2-d)} (C_d \text{Vol}(\mathcal{M}))^{2/(2-d)} \rceil \quad (14)$$

such that, for all $k > N_1$, it holds that

$$\lambda_{k+1} - \lambda_k \leq \alpha.$$

Proof. This is a direct consequence of Weyl's law [1]. □

Given this asymptotic behavior, a finite partition can be obtained by putting eigenvalues that are less than $\alpha > 0$ apart from each other in groups. This spectrum separation strategy is formalized in Definition 2. To achieve this, we use filters acting in the spectral domain called Frequency Difference Threshold (FDT) filters, which are introduced in Definition 3.

Definition 2 (α -separated spectrum). The α -separated spectrum of a LB operator \mathcal{L} is defined as the partition $\Lambda_1(\alpha) \cup \dots \cup \Lambda_N(\alpha)$ such that, all $\lambda_i \in \Lambda_k(\alpha)$ and $\lambda_j \in \Lambda_l(\alpha)$, $k \neq l$, satisfy

$$|\lambda_i - \lambda_j| > \alpha.$$

Definition 3 (α -FDT filter). The α -frequency difference threshold (α -FDT) filter is defined as a filter $\mathbf{h}(\mathcal{L})$ whose frequency response satisfies

$$|h(\lambda_i) - h(\lambda_j)| \leq \Delta_k \text{ for all } \lambda_i, \lambda_j \in \Lambda_k(\alpha) \quad (15)$$

while $\Delta_k \leq \Delta$ for $k = 1, \dots, N$.

In α -separated spectrum, eigenvalues $\lambda_i \in \Lambda_k(\alpha)$ and $\lambda_j \in \Lambda_l(\alpha)$ in different sets ($k \neq l$) are at least α apart from each other. Conversely, eigenvalues $\lambda_i, \lambda_j \in \Lambda_k(\alpha)$ are no more than α away from each other. This creates several eigenvalue groups spaced by at least α . Note that $\Lambda_k(\alpha)$ may be a singleton, i.e., it can be formed by a single eigenvalue that is at least α away from all of its neighboring eigenvalues. The partitioning of the spectrum defined in Definition 2 can be achieved by an α -FDT filter, which separates the spectrum by assigning similar frequency responses that deviate no more than Δ_k from each other to eigenvalues $\lambda_i \in \Lambda_k(\alpha)$, $1 \leq k \leq N$. In other words, for eigenvalues $\lambda_i, \lambda_j \in \Lambda_k(\alpha)$, the α -FDT filter does not discriminate them to realize the separation of the spectrum. The difference bounds Δ_k are finite so that they can be bounded by some Δ .

To obtain MNNs that are stable to absolute perturbations of \mathcal{L} , we also need these filters to be Lipschitz continuous as introduced in Definition 4.

Definition 4 (Lipschitz filter). A filter is A_h -Lipschitz if its frequency response is Lipschitz continuous with constant A_h , i.e.,

$$|h(a) - h(b)| \leq A_h |a - b| \text{ for all } a, b. \quad (16)$$

Between groups, the filters we consider are thus Lipschitz continuous with Lipschitz constant A_h . Hence, in regions of the spectrum where the $\Lambda_k(\alpha)$ are singletons, the filter can vary with slope at most A_h as shown in Figure 1a. While the $h(\lambda)$ in Definition 3 is constrained, we can still find some A_h to construct such a filter in the form of (8).

Under mild assumptions on the amplitude of the filters h (Assumption 2) and on the nonlinearities of the MNN (Assumption 3), it can be shown that MNNs constructed with Lipschitz continuous α -FDT filters are stable to absolute perturbations of the LB operator. This result is stated in Theorem 3. The proof is deferred to the appendices.

Assumption 2 (Non-amplifying filters). The filter function $h : \mathbb{R} \rightarrow \mathbb{R}$ is non-amplifying. I.e., for all λ , h satisfies $|h(\lambda)| \leq 1$.

Assumption 3 (Normalized Lipschitz activation functions). The activation function σ is normalized Lipschitz continuous, i.e., $|\sigma(a) - \sigma(b)| \leq |a - b|$, with $\sigma(0) = 0$.

Note that the above assumptions are rather reasonable, as the filter function $h(\lambda)$ can easily be scaled and most common activation functions (e.g., the ReLU, the modulus and the sigmoid) are normalized Lipschitz by design.

Theorem 3 (MNN stability to absolute perturbations). Consider a manifold \mathcal{M} with LB operator \mathcal{L} . Let $\Phi(\mathbf{H}, \mathcal{L}, f)$ be an L -layer MNN on \mathcal{M} (10) with $F_0 = F_L = 1$ input and output features and $F_i = F$, $i = 1, 2, \dots, L-1$ features per layer. The filters $\mathbf{h}(\mathcal{L})$ are α -FDT filters [cf. Definition 3] and A_h -Lipschitz [cf. Definition 4]. Consider an absolute perturbation $\mathcal{L}' = \mathcal{L} + \mathbf{A}$ of the LB operator \mathcal{L} [cf. Definition 1] where $\|\mathbf{A}\| = \epsilon < \alpha$. Then, under Assumptions 2 and 3 it holds that

$$\|\Phi(\mathbf{H}, \mathcal{L}, f) - \Phi(\mathbf{H}, \mathcal{L}', f)\|^2 \leq L F^{L-1} \left(\frac{\pi^2 (N_s + 1) \epsilon^2}{4(\alpha - \epsilon)^2} + A_h^2 \epsilon^2 + 4(N - N_s) \Delta^2 \right) \|f\|^2, \quad (17)$$

where N is the size of the partition that defines the α -separated spectrum [cf. Definition 2] and N_s is the number of singleton partitions.

Corollary 1. By setting the frequency response difference bound $\Delta = \pi\epsilon/(4\alpha - 4\epsilon)$, the result under the same condition in Theorem 3 can be written as

$$\|\Phi(\mathbf{H}, \mathcal{L}, f) - \Phi(\mathbf{H}, \mathcal{L}', f)\|^2 \leq L F^{L-1} \left(\frac{\pi^2 (N + 1) \epsilon^2}{4(\alpha - \epsilon)^2} + A_h^2 \epsilon^2 \right) \|f\|^2. \quad (18)$$

For $\epsilon \ll \alpha$, the denominator on the right hand side of (17) is close to $4\alpha^2$. Thus, MNNs with α -FDT Lipschitz filters are stable to absolute perturbations. The stability bound in Theorem 3 depends on the number of layers L and the number of features per layer F of the MNN, which is expected due

to the cascading structure. It also depends on the continuity of the filter function $h(\lambda)$, which is measured by constant A_h , and on the frequency difference threshold α , which affects the stability bound directly and indirectly through the size of the partition N . As detailed in the proof of this theorem, the terms in this stability arise from perturbations of the eigenvalues λ_i as well as the eigenfunctions ϕ_i . The influence of the eigenvalue perturbations is more intuitive as the frequency response $h(\lambda)$ is evaluated at the λ_i . The perturbations of the eigenfunctions affect the bound by changing projection directions.

From Corollary 1 which is a particular case of Theorem 3, we conclude that in order to improve stability it is necessary to have a small Lipschitz constant A_h and a large frequency difference threshold α . A smaller constant A_h leads to a smoother filter function, which in turn leads to more similar frequency responses to different eigenvalues. A larger threshold α would make for fewer sets $\Lambda_k(\alpha)$, which decreases the cardinality N . Eigenvalues that would otherwise belong to singletons for smaller α would now be grouped. While this could lead to an increase in the number of sets with more than one eigenvalue, N will either stay the same or decrease because the number of eigenvalues would not exceed the number of groups [cf. Proposition 1]. Therefore, a smaller constant A_h and a larger threshold α both lead to larger stability, but this happens at the cost of the discriminability of the filters and hence of the MNN. In giving similar responses to all spectral components, a smoother filter function becomes less discriminative. In grouping more eigenvalues together, a filter with larger frequency difference threshold treats more eigenvalues with little difference. This reveals a stability-discriminability trade-off where discriminability is understood as the ability to tell frequencies apart wherever they are in the spectrum. Importantly, this trade-off is not related to the magnitude of the frequencies that the filters amplify.

3.2 Stability to Relative Perturbations of \mathcal{L}

Next we study MNN stability to relative perturbations of the LB operator defined as follows.

Definition 5 (Relative perturbations). Let \mathcal{L} be the LB operator of manifold \mathcal{M} . A relative perturbation of \mathcal{L} is defined as

$$\mathcal{L}' - \mathcal{L} = \mathbf{E}\mathcal{L}, \quad (19)$$

where the relative perturbation operator \mathbf{E} is symmetric.

Relative perturbations of the LB operator are additive perturbations but where the perturbation operator is now multiplicative. In particular, note that the relative perturbation in Definition 5 can be expressed as an absolute perturbation [cf. Definition 1] where $\mathbf{A} = \mathbf{E}\mathcal{L}$.

Like absolute perturbations, relative perturbations lead to shifts of the eigenvalues and eigenfunctions of \mathcal{L} . Proposition 1 again allows us to split the infinite-dimensional spectrum into a finite number of groups. In the case of relative perturbations, the perturbations to the eigenvalues are proportional to their absolute value [cf. Lemma 3 in the supplementary material]. Hence, to enforce stability we need to separate the spectrum relatively to the ratio between neighboring eigenvalues. This partitioning, which we call the γ -separated spectrum, is described in Definition 6. The γ -separated spectrum is achieved by so-called Frequency Ratio Threshold (FRT) filters, which operate in the spectral domain. They are introduced in Definition 7.

Definition 6 (γ -separated spectrum.). The γ -separated spectrum of a LB operator \mathcal{L} is defined as the partition $\Lambda_1(\gamma) \cup \dots \cup \Lambda_M(\gamma)$ such that, all $\lambda_i \in \Lambda_k(\gamma)$ and $\lambda_j \in \Lambda_l(\gamma)$, $k \neq l$, satisfy

$$\left| \frac{\lambda_i}{\lambda_j} - 1 \right| > \gamma. \quad (20)$$

Definition 7 (γ -FRT filter.). The γ -frequency ratio threshold (γ -FRT) filter is a filter $\mathbf{h}(\mathcal{L})$ whose frequency response satisfies

$$|h(\lambda_i) - h(\lambda_j)| \leq \Delta_k, \text{ for all } \lambda_i, \lambda_j \in \Lambda_k(\gamma) \quad (21)$$

while $\Delta_k \leq \Delta$ for $k = 1, 2, \dots, M$.

In the γ -separated spectrum in Definition 6, eigenvalues $\lambda_j \in \Lambda_k(\gamma)$ and $\lambda_i \in \Lambda_l(\gamma)$ in different groups ($k \neq l$) are at least $\gamma \min(\lambda_i, \lambda_j)$ apart from one another. This means that, for $\lambda_i, \lambda_{i+1} \in \Lambda_k(\gamma)$, $\lambda_{i+1} - \lambda_i \leq \gamma \lambda_i$. In other words, the sets $\Lambda_k(\gamma)$ are built based on eigenvalue distances relative to the eigenvalues' magnitudes weighted by the filter parameter γ .

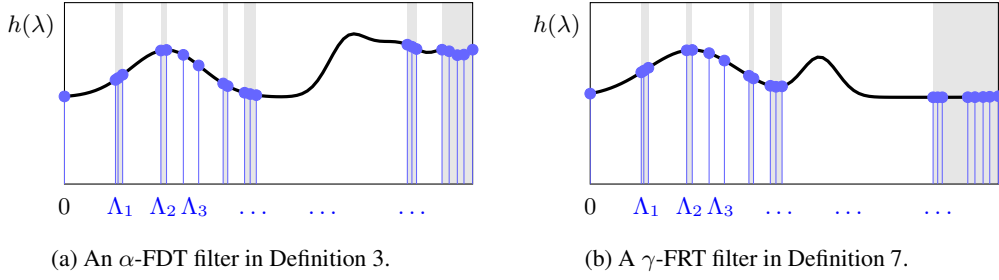


Figure 1: Illustrations of FDT and FRT filters. The x -axis stands for the spectrum with each sample representing an eigenvalue. The gray shade shows the grouping of the eigenvalues. As we can see, the α -FDT filter varies freely (i.e. with slope at most A_h) between groups while changes little for eigenvalues in the same group. When eigenvalues are large enough, α -FDT filter tends to oscillate around a certain value while γ -FRT filter tends to be flat.

Just like α -FDT filters help form the α -separated spectrum in the case of absolute perturbations, the γ -FRT filter in Definition 7 partitions the spectrum into a γ -separated spectrum. I.e., γ -FRT filters treat eigenvalues $\lambda_i, \lambda_j \in \Lambda_k(\gamma)$ as similar by giving them responses with bounded difference, whereas eigenvalues belonging to different sets $\Lambda_k(\gamma)$ and $\Lambda_l(\gamma)$, $k \neq l$, are treated independently.

To achieve MNNs that are stable to relative perturbations of the LB operator, we also need their filters h to satisfy an *integral Lipschitz* condition on the rate of change of their frequency responses.

Definition 8 (Integral Lipschitz filter). A filter is integral Lipschitz with constant B_h if its frequency response is given by

$$|h(a) - h(b)| \leq \frac{B_h |a - b|}{(a + b)/2} \text{ for all } a, b. \quad (22)$$

The integral Lipschitz condition can be interpreted as demanding the filter functions to be Lipschitz continuous on the interval (a, b) with a Lipschitz constant $2B_h/(a + b)$. When a and b are close, this condition can be approximated by $|ah'(a)| \leq B_h$, which means that the filter function flattens when the frequencies (i.e., the eigenvalues) are high as is shown in Figure 1b.

Under the same assumptions on the filter amplitude and on the activation function as in the previous section (Assumptions 2 and 3), MNNs constructed with banks of γ -FRT filters that are integral Lipschitz are stable to relative perturbations as stated in Theorem 4. The proof is deferred to the supplementary material.

Theorem 4 (MNN stability to relative perturbations). Let \mathcal{M} be a manifold with LB operator \mathcal{L} . Let f be manifold data and $\Phi(\mathbf{H}, \mathcal{L}, f)$ an L -layer MNN on \mathcal{M} (10) with $F_0 = F_L = 1$ input and output features and $F_l = F, l = 1, 2, \dots, L-1$ features per layer, and where the filters $\mathbf{h}(\mathcal{L})$ are γ -FRT filters with $\Delta = \pi\epsilon/(2\gamma - 2\epsilon + 2\gamma\epsilon)$ [cf. Definition 7] and B_h -integral Lipschitz [cf. Definition 8]. Consider a relative perturbation $\mathcal{L}' = \mathcal{L} + \mathbf{E}\mathcal{L}$ of the LB operator \mathcal{L} [cf. Definition 5] where $\|\mathbf{E}\| = \epsilon < \gamma$. Then, under Assumptions 2 and 3 it holds that

$$\|\Phi(\mathbf{H}, \mathcal{L}, f) - \Phi(\mathbf{H}, \mathcal{L}', f)\|^2 \leq LF^{L-1} \left(\frac{\pi^2(M+1)\epsilon^2}{(\gamma - \epsilon + \gamma\epsilon)^2} + \left(\frac{2B_h\epsilon}{2-\epsilon} \right)^2 \right) \|f\|^2, \quad (23)$$

where M is the size of the partition that defines the γ -separated spectrum [cf. Definition 6].

When ϵ is sufficiently small ($\epsilon \ll \min(\gamma, 2)$), which is typically the case with deformations such as the one in Theorem 2), the denominators on the right hand side of (23) are approximately equal to γ^2 and 4 respectively. Thus, MNNs with γ -FRT integral Lipschitz filters are stable to relative perturbations of the LB operator. The frequency ratio threshold γ affects stability directly (by appearing in the bound in Theorem 4) and indirectly through the partition size M . With a larger γ , fewer eigenvalues will be in singletons, thus decreasing M and improving stability. A smaller integral Lipschitz constant B_h also increases stability. However, small B_h and large γ make for smoother filters which in turn lead to a less discriminative neural network. Therefore, MNNs with integral Lipschitz γ -FRT filters also exhibit a trade-off between discriminability and stability.

Together, Theorems 2, 3 and 4 imply that MNNs are stable to the manifold deformations v introduced in the beginning of this section. This is because these deformations spawn a perturbation of the LB operator that consists of both an absolute and a relative perturbation. For stability to hold, the filters that make up the layers of the MNN need to be α -FDT [cf. Definition 3], γ -FRT [cf. Definition 7], Lipschitz [cf. Definition 4] and integral Lipschitz [cf. Definition 8]. The requirement that the filter be α -FDT can be removed as long as $\lambda_1 > 0$ and $\gamma = \alpha/\lambda_1$, since a α/λ_1 -FRT filter is always α -FDT. This result is stated in simplified form in Theorem 1. The complete statement can be found in the supplementary material.

4 Numerical Experiments

We take GNNs as discretizations of MNNs to help verify our results. By constructing a graph model to represent the wireless adhoc network structure, we can solve the optimal resource allocation problem with a GNN. We consider a wireless adhoc network with $n = 50$ pairs of transmitters and receivers within a range of $[-50m, 50m]^2$, i.e., the transmitter density is $\rho = 0.02$ transmitter/ m^2 . The receiver $r(i)$ is paired with the transmitter i by dropping randomly around the transmitter. The channel link state between each transmitter and receiver is denoted $[\mathbf{S}(t)]_{ij} := s_{ij}(t) \in \mathbb{R}_+$ at time t between transmitter i and receiver $r(j)$. Here, we focus on the power allocation problem among n transmitters over an AWGN channel with interference, with $\mathbf{p}(\mathbf{S}) = [p_1(\mathbf{S}), p_2(\mathbf{S}), \dots, p_n(\mathbf{S})]$ denoting the power allocated to each transmitter under channel condition \mathbf{S} . The Shannon channel rate of transmitter i is represented as f_i . The goal is to maximize the sum rate capacity under a total power budget P_{max} . The problem can be formulated as an optimization problem as

$$f^* = \max_{\mathbf{p}(\mathbf{S})} \sum_{i=1}^n f_i \quad \text{s.t.} \quad r_i = \mathbb{E} \left[\log \left(1 + \frac{s_{ii}^2 p_i(\mathbf{S})}{1 + \sum_{j \neq i} s_{ij}^2 p_j(\mathbf{S})} \right) \right],$$

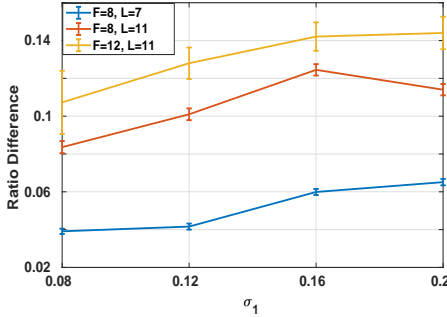
$$\mathbb{E}[\mathbf{1}^T \mathbf{p}] \leq P_{max}, \quad p_i(\mathbf{S}) \in \{0, p_0\}.$$

With the transmitters and receivers modeled as graph nodes, the links between each transmitter and receiver can therefore be seen as edges. The channel matrix \mathbf{S} composed of link conditions can be seen as the graph shift operator. In the real world, the distribution of the transmitters can vary, which can be seen as a deformation to the underlying manifold. To capture this, we model the deformation by changing the density and the location distribution of the transmitters respectively.

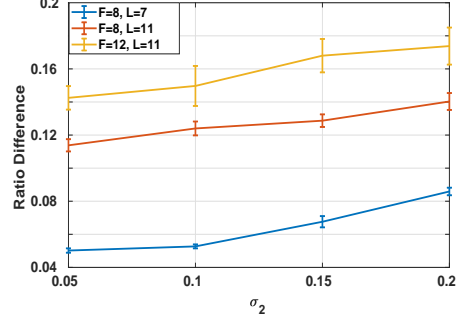
We measure policy performance in terms of the ratio of the sum-of-rate achieved by the GNN and a baseline heuristic method (WMMSE [18]) after training for 40,000 iterations (details on hyperparameters and other settings can be found in the appendices). We observe that the sum of capacity converges and the trained GNN can achieve the optimal power allocation policy on the original graph. By employing the same GNN (i.e., with the same parameters) on the deformed graph, we measure stability by computing the difference between the ratios achieved in the original wireless network setting and in the deformed settings described in the caption of Figure 2. In this figure, we see that this difference increases when the perturbations become larger, but overall the differences are small. We also compare GNNs with different architectures, and observe that deeper and wider GNNs are less stable. Both of these observations validate our stability results.

5 Conclusions

In this paper, we have defined manifold convolutions and manifold neural networks. We prove that the deformations on the Riemannian manifolds can be represented as a form of perturbations to the Laplace-Beltrami operator. Considering the infinite dimensionality of Laplace-Beltrami operators, we import the definition of frequency dependent filters to help separate the spectrum. By assigning similar frequency responses to the eigenvalues that are close enough, these filters can build up a manifold neural network architecture that can be proved to be stable to absolute and relative perturbations to the Laplace-Beltrami operators. We conclude that the manifold neural networks are thus stable to deformations. We finally verified our results numerically with a power allocation problem in wireless adhoc networks. In the future, we will carry out simulations on real-world datasets to be more comprehensive.



(a) Stability to varying density.



(b) Stability to mixed uniform distributions.

Figure 2: Difference between the sum-of-rate ratios on the original wireless network setting and the deformed one. The x axis in Figure 2a stands for the change on transmitter density, i.e., the perturbed density is given by $\rho' = \rho/(1-\sigma_1)$. In Figure 2b, the x -axis measures the perturbation to the original uniform distribution of the transmitters' locations. In the range $[-50m, 0]$, a transmitter is dropped with probability $(1 + \sigma_2)/2$, and in $[0, 50m]$, with probability $(1 - \sigma_2)/2$ on each direction.

References

- [1] W. Arendt, R. Nittka, W. Peter, and F. Steiner. Weyl's law: Spectral properties of the laplacian in mathematics and physics. *Mathematical analysis of evolution, information, and complexity*, pages 1–71, 2009.
- [2] M. M. Bronstein, J. Bruna, Y. LeCun, A. Szlam, and P. Vandergheynst. Geometric deep learning: going beyond euclidean data. *IEEE Signal Processing Magazine*, 34(4):18–42, 2017.
- [3] M. M. Bronstein, J. Bruna, T. Cohen, and P. Veličković. Geometric deep learning: Grids, groups, graphs, geodesics, and gauges. *arXiv preprint arXiv:2104.13478*, 2021.
- [4] A. Chowdhury, G. Verma, C. Rao, A. Swami, and S. Segarra. Unfolding wmmse using graph neural networks for efficient power allocation. *IEEE Transactions on Wireless Communications*, 2021.
- [5] W. Fan, Y. Ma, Q. Li, Y. He, E. Zhao, J. Tang, and D. Yin. Graph neural networks for social recommendation. In *The World Wide Web Conference*, pages 417–426, 2019.
- [6] F. Gama, A. G. Marques, G. Leus, and A. Ribeiro. Convolutional neural network architectures for signals supported on graphs. *IEEE Transactions on Signal Processing*, 67(4):1034–1049, 2019.
- [7] F. Gama, A. Ribeiro, and J. Bruna. Stability of graph scattering transforms. *Advances in Neural Information Processing Systems*, 32:8038–8048, 2019.
- [8] F. Gama, J. Bruna, and A. Ribeiro. Stability properties of graph neural networks. *IEEE Transactions on Signal Processing*, 68:5680–5695, 2020.
- [9] N. Keriven, A. Bietti, and S. Vaienti. Convergence and stability of graph convolutional networks on large random graphs. *arXiv preprint arXiv:2006.01868*, 2020.
- [10] R. Levie, M. M. Bronstein, and G. Kutyniok. Transferability of spectral graph convolutional neural networks. *arXiv preprint arXiv:1907.12972*, 2019.
- [11] S. Mallat. Group invariant scattering. *Communications on Pure and Applied Mathematics*, 65(10):1331–1398, 2012.
- [12] A. Parada-Mayorga and A. Ribeiro. Algebraic neural networks: Stability to deformations. *arXiv preprint arXiv:2009.01433*, 2020.
- [13] S. Rosenberg and R. Steven. *The Laplacian on a Riemannian manifold: an introduction to analysis on manifolds*. Number 31. Cambridge University Press, 1997.

- [14] L. Ruiz, Z. Wang, and A. Ribeiro. Graph and graphon neural network stability. *arXiv preprint arXiv:2010.12529*, 2020.
- [15] L. Ruiz, F. Gama, and A. Ribeiro. Graph neural networks: Architectures, stability, and transferability. *Proceedings of the IEEE*, 109(5):660–682, 2021.
- [16] F. Scarselli, M. Gori, A. C. Tsoi, M. Hagenbuchner, and G. Monfardini. The graph neural network model. *IEEE transactions on neural networks*, 20(1):61–80, 2008.
- [17] A. Seelmann. Notes on the $\sin 2\theta$ theorem. *Integral Equations and Operator Theory*, 79(4):579–597, 2014.
- [18] Q. Shi, M. Razaviyayn, Z.-Q. Luo, and C. He. An iteratively weighted mmse approach to distributed sum-utility maximization for a mimo interfering broadcast channel. *IEEE Transactions on Signal Processing*, 59(9):4331–4340, 2011.
- [19] G. K. Smyth. Polynomial approximation. *Wiley StatsRef: Statistics Reference Online*, 2014.
- [20] S. Verma and Z.-L. Zhang. Stability and generalization of graph convolutional neural networks. In *Proceedings of the 25th ACM SIGKDD International Conference on Knowledge Discovery & Data Mining*, pages 1539–1548, 2019.
- [21] Z. Wang, M. Eisen, and A. Ribeiro. Unsupervised learning for asynchronous resource allocation in ad-hoc wireless networks. *arXiv preprint arXiv:2011.02644*, 2020.
- [22] S. Wu, Y. Tang, Y. Zhu, L. Wang, X. Xie, and T. Tan. Session-based recommendation with graph neural networks. In *Proceedings of the AAAI Conference on Artificial Intelligence*, volume 33, pages 346–353, 2019.
- [23] J. Zhou, G. Cui, S. Hu, Z. Zhang, C. Yang, Z. Liu, L. Wang, C. Li, and M. Sun. Graph neural networks: A review of methods and applications. *AI Open*, 1:57–81, 2020.
- [24] D. Zou and G. Lerman. Graph convolutional neural networks via scattering. *Applied and Computational Harmonic Analysis*, 49(3):1046–1074, 2020.

A Appendix

A.1 Proof of Theorem 2

Proof. Based on equation (11) and the definition of Laplace operator in (1), the operation carried out on the deformed manifold data f can be written as

$$-\mathcal{L}'f(x) = \langle \nabla, \nabla \rangle f(v(x)) = \langle \nabla v(x)^T \nabla_v, \nabla v(x)^T \nabla_v \rangle f(v(x)). \quad (24)$$

The equality in (24) results from the chain rule of gradient operator where ∇_v is denoted as the intrinsic gradient around $v(x)$ in the tangent space $T_{v(x)}\mathcal{M}$. By replacing ∇_v with $(\nabla_v - \nabla) + \nabla$ and $\nabla v(x) = 1 + \nabla \tau(x)$ the inner product term in (24) can be rewritten as

$$\langle \nabla v(x)^T \nabla_v, \nabla v(x)^T \nabla_v \rangle = \langle \nabla, \nabla \rangle + 2\langle \nabla \tau(x)^T \nabla, \nabla \rangle + \langle \nabla \tau(x)^T \nabla, \nabla \tau(x)^T \nabla \rangle + \mathbf{A}_2, \quad (25)$$

with \mathbf{A}_2 contains $\nabla_v - \nabla$ term. Due to the smoothness of the manifold stated in Assumption 1, $\|\nabla_v - \nabla\| \leq \|\tau(x)\|$ with $v(x) = x + \tau(x)$. This leads to the norm of \mathbf{A}_2 bounded as $\|\mathbf{A}_2\| = O(\|\tau(x)\|)$. With $\mathcal{L} = -\langle \nabla, \nabla \rangle$, the perturbed operator can be further written as

$$\mathcal{L} - \mathcal{L}' = 2\langle \nabla \tau(x)^T \nabla, \nabla \rangle + \langle \nabla \tau(x)^T \nabla, \nabla \tau(x)^T \nabla \rangle + \mathbf{A}_2 \quad (26)$$

$$= \langle \nabla \tau(x), \nabla \tau(x) \rangle \langle \nabla, \nabla \rangle + 2\|\nabla \tau(x)\| \langle \nabla, \nabla \rangle + \mathbf{A}_1 + \mathbf{A}_2. \quad (27)$$

From (26) to (27), we extract the relative term and use \mathbf{A}_1 to represent the compliment terms. This leads to

$$\mathbf{E} = \langle \nabla \tau(x), \nabla \tau(x) \rangle + 2\|\nabla \tau(x)\|, \quad (28)$$

as the relative perturbation term, the norm of which is bounded by the leading term as $O(\epsilon)$. The norm of the compliment term therefore can be written as

$$\|\mathbf{A}_1\| = \|\mathbf{E} \langle \nabla, \nabla \rangle - 2\langle \nabla \tau(x)^T \nabla, \nabla \rangle - \langle \nabla \tau(x)^T \nabla, \nabla \tau(x)^T \nabla \rangle\| \quad (29)$$

$$\leq \|2\|\nabla \tau(x)\| \|\nabla\|^2 - 2\langle \nabla \tau(x)^T \nabla, \nabla \rangle\| + \| \|\nabla \tau(x)\|^2 \|\nabla\|^2 - \|\nabla \tau(x)\nabla\|^2 \|, \quad (30)$$

which can be also bounded by the leading terms as $O(\epsilon)$ combining with Assumption 1 that $\|\nabla\| \leq 1$.

□

A.2 Proof of Theorem 3

Proof. We start by bounding the norm difference between two outputs of filter functions on operators \mathcal{L} and \mathcal{L}' defined in (9) as

$$\|\mathbf{h}(\mathcal{L})f - \mathbf{h}(\mathcal{L}')f\|^2 = \left\| \sum_{i=1}^{\infty} h(\lambda_i) \langle f, \phi_i \rangle \phi_i - \sum_{i=1}^{\infty} h(\lambda'_i) \langle f, \phi'_i \rangle \phi'_i \right\|^2 \quad (31)$$

We denote the index of partitions that contain a single eigenvalue as a set \mathcal{K}_s and the rest as a set \mathcal{K}_m . We can decompose the filter function as $h(\lambda) = h^{(0)}(\lambda) + \sum_{l \in \mathcal{K}_m} h^{(l)}(\lambda)$ with

$$h^{(0)}(\lambda) = \begin{cases} h(\lambda) - \sum_{l \in \mathcal{K}_m} h(C_l) & \lambda \in [\Lambda_k(\alpha)]_{k \in \mathcal{K}_s} \\ 0 & \text{otherwise} \end{cases} \quad \text{and} \quad (32)$$

$$h^{(l)}(\lambda) = \begin{cases} h(C_l) & \lambda \in [\Lambda_k(\alpha)]_{k \in \mathcal{K}_s} \\ h(\lambda) & \lambda \in \Lambda_l(\alpha) \\ 0 & \text{otherwise} \end{cases} \quad (33)$$

where C_l is some constant in $\Lambda_l(\alpha)$. We can start by analyzing the output difference of $h^{(0)}(\lambda)$. With the triangle inequality, the norm difference can then be written as

$$\begin{aligned} & \left\| \sum_{i=1}^{\infty} h^{(0)}(\lambda_i) \langle f, \phi_i \rangle \phi_i - h^{(0)}(\lambda'_i) \langle f, \phi'_i \rangle \phi'_i \right\|^2 \\ &= \left\| \sum_{i=1}^{\infty} h^{(0)}(\lambda_i) \langle f, \phi_i \rangle \phi_i - h^{(0)}(\lambda_i) \langle f, \phi'_i \rangle \phi'_i + h^{(0)}(\lambda_i) \langle f, \phi'_i \rangle \phi'_i - h^{(0)}(\lambda'_i) \langle f, \phi'_i \rangle \phi'_i \right\|^2 \quad (34) \end{aligned}$$

$$\leq \left\| \sum_{i=1}^{\infty} h^{(0)}(\lambda_i) \langle f, \phi_i \rangle \phi_i - h^{(0)}(\lambda_i) \langle f, \phi'_i \rangle \phi'_i \right\|^2 + \left\| \sum_{i=1}^{\infty} h^{(0)}(\lambda_i) \langle f, \phi'_i \rangle \phi'_i - h^{(0)}(\lambda'_i) \langle f, \phi'_i \rangle \phi'_i \right\|^2 \quad (35)$$

$$\begin{aligned} & \leq \left\| \sum_{i=1}^{\infty} h^{(0)}(\lambda_i) (\langle f, \phi_i \rangle \phi_i - \langle f, \phi_i \rangle \phi'_i + \langle f, \phi_i \rangle \phi'_i - \langle f, \phi'_i \rangle \phi'_i) \right\|^2 \\ & \quad + \left\| \sum_{i=1}^{\infty} (h^{(0)}(\lambda_i) - h^{(0)}(\lambda'_i)) \langle f, \phi'_i \rangle \phi'_i \right\|^2 \quad (36) \end{aligned}$$

$$\begin{aligned} & \leq \left\| \sum_{i=1}^{\infty} h^{(0)}(\lambda_i) \langle f, \phi_i \rangle (\phi_i - \phi'_i) \right\|^2 + \left\| \sum_{i=1}^{\infty} h^{(0)}(\lambda_i) \langle f, \phi_i - \phi'_i \rangle \phi'_i \right\|^2 \\ & \quad + \left\| \sum_{i=1}^{\infty} (h^{(0)}(\lambda_i) - h^{(0)}(\lambda'_i)) \langle f, \phi'_i \rangle \phi'_i \right\|^2 \quad (37) \end{aligned}$$

$$\begin{aligned} & \leq \sum_{i=1}^{\infty} |h^{(0)}(\lambda_i)|^2 \langle f, \phi_i \rangle^2 \|\phi_i - \phi'_i\|^2 + \sum_{i=1}^{\infty} |h^{(0)}(\lambda_i)|^2 \|\phi_i - \phi'_i\|^2 \|f\|^2 \\ & \quad + \sum_{i=1}^{\infty} |h^{(0)}(\lambda_i) - h^{(0)}(\lambda'_i)|^2 \langle f, \phi'_i \rangle^2. \quad (38) \end{aligned}$$

From equation (37) to equation (38), we use the orthonormal property that $\|\phi_i\| = 1$ for all i .

Now we need to include two important lemmas to analyze the influence on eigenvalues and eigenfunctions caused by the perturbation.

Lemma 1. [Weyl's Theorem] The eigenvalues of LB operators \mathcal{L} and perturbed $\mathcal{L}' = \mathcal{L} + \mathbf{A}$ satisfy

$$|\lambda_i - \lambda'_i| \leq \|\mathbf{A}\|, \text{ for all } i = 1, 2 \dots \quad (39)$$

Proof of Lemma 1. The minimax principle asserts that

$$\lambda_i(\mathcal{L}) = \max_{\text{codim } T \leq i-1} \lambda[\mathcal{L}, T] = \max_{\text{codim } T \leq i-1} \min_{u \in T, \|u\|=1} \langle \mathcal{L}u, u \rangle. \quad (40)$$

Then for any $1 \leq k$, we have

$$\lambda_i(\mathcal{L}') = \max_{\text{codim } T \leq i-1} \min_{u \in T, \|u\|=1} \langle (\mathcal{L} + \mathbf{A})u, u \rangle \quad (41)$$

$$= \max_{\text{codim } T \leq i-1} \min_{u \in T, \|u\|=1} (\langle \mathcal{L}u, u \rangle + \langle \mathbf{A}u, u \rangle) \quad (42)$$

$$\geq \max_{\text{codim } T \leq i-1} \min_{u \in T, \|u\|=1} \langle \mathcal{L}u, u \rangle + \lambda_1(\mathbf{A}) \quad (43)$$

$$= \lambda_1(\mathbf{A}) + \max_{\text{codim } T \leq i-1} \min_{u \in T, \|u\|=1} \langle \mathcal{S}u, u \rangle \quad (44)$$

$$= \lambda_k(\mathcal{S}) + \lambda_1(\mathbf{A}). \quad (45)$$

Similarly, we can have $\lambda_i(\mathcal{L}') \leq \lambda_i(\mathcal{L}) + \max_k \lambda_k(\mathbf{A})$. This leads to $\lambda_1(\mathbf{A}) \leq \lambda_i(\mathcal{S} + \mathbf{A}) - \lambda_k(\mathcal{S}) \leq \max_k \lambda_k(\mathbf{A})$. This leads to the conclusion that:

$$|\lambda'_i - \lambda_i| \leq \|\mathbf{A}\|. \quad (46)$$

□

To measure the difference of eigenfunctions, we introduce the Davis-Kahan $\sin \theta$ theorem as follows.

Lemma 2 (Davis-Kahan $\sin \theta$ Theorem). Suppose the spectra of operators \mathcal{L} and \mathcal{L}' are partitioned as $\sigma \cup \Sigma$ and $\omega \cup \Omega$ respectively, with $\sigma \cap \Sigma = \emptyset$ and $\omega \cap \Omega = \emptyset$. Then we have

$$\|E_{\mathcal{L}}(\sigma) - E_{\mathcal{L}'}(\omega)\| \leq \frac{\pi}{2} \frac{\|(\mathcal{L}' - \mathcal{L})E_{\mathcal{L}}(\sigma)\|}{d} \leq \frac{\pi}{2} \frac{\|\mathcal{L}' - \mathcal{L}\|}{d}, \quad (47)$$

where d satisfies $\min_{x \in \sigma, y \in \Omega} |x - y| \geq d$ and $\min_{x \in \Sigma, y \in \omega} |x - y| \geq d$.

Proof of Lemma 2. See [17]. \square

For the first term in (38), we employ Lemma 2 and therefore we have $\sigma = \lambda_i$ and $\omega = \lambda'_i$, for $\lambda_i \in [\Lambda_k(\alpha)]_{k \in \mathcal{K}_s}$ we can have

$$\|\phi_i - \phi'_i\| \leq \frac{\pi}{2} \frac{\|\mathbf{A}\|}{\alpha - \epsilon} = \frac{\pi}{2} \frac{\epsilon}{\alpha - \epsilon}. \quad (48)$$

Here d can be seen as $d = \min_{\lambda_i \in \Lambda_k(\alpha), \lambda_j \in \Lambda_l(\alpha), k \neq l} |\lambda_i - \lambda'_j|$. Combined with the fact that $|\lambda_i - \lambda_j| > \alpha$ and $|\lambda_i - \lambda'_i| \leq \epsilon$ for all $\lambda_i \in \Lambda_k(\alpha), \lambda_j \in \Lambda_l(\alpha), k \neq l$, we have $d \geq \alpha - \epsilon$. With the definition of $\|f\|^2 = \sum_i \langle f, \phi_i \rangle^2 = \sum_i \langle f, \phi'_i \rangle^2$, we have the first term in (38) bounded as

$$\sum_{i=1}^{\infty} |h^{(0)}(\lambda_i)|^2 \langle f, \phi_i \rangle^2 \|\phi_i - \phi'_i\|^2 \leq \left(\frac{\pi \epsilon}{2(\alpha - \epsilon)} \right)^2 \|f\|^2. \quad (49)$$

The second term in (38) is bounded as

$$\sum_{i=1}^{\infty} |h^{(0)}(\lambda_i)|^2 \|\phi_i - \phi'_i\|^2 \leq N_s \left(\frac{\pi \epsilon}{2(\alpha - \epsilon)} \right)^2 \|f\|^2. \quad (50)$$

These two bounds are obtained by noting that $|h^{(0)}(\lambda)| < 1$ and $h^{(0)}(\lambda) = 0$ for $\lambda \in [\Lambda_k(\alpha)]_{k \in \mathcal{K}_m}$. The number of eigenvalues within $[\Lambda_k(\alpha)]_{k \in \mathcal{K}_s}$ is denoted as N_s . The third term in (38) can be bounded by the Lipschitz continuity of h combined with Lemma 1.

$$\sum_{i=1}^{\infty} |h^{(0)}(\lambda_i) - h^{(0)}(\lambda'_i)|^2 \langle f, \phi'_i \rangle^2 \leq \sum_{i=1}^{\infty} A_h^2 |\lambda_i - \lambda'_i|^2 \langle f, \phi'_i \rangle^2 \leq A_h^2 \epsilon^2 \|f\|^2. \quad (51)$$

Then we need to analyze the output difference of $h^{(l)}(\lambda)$, we can bound this as

$$\left\| \mathbf{h}^{(l)}(\mathcal{L})f - \mathbf{h}^{(l)}(\mathcal{L}')f \right\|^2 \leq \|(h(C_l) + \Delta)f - (h(C_l) - \Delta)f\|^2 \leq 4\Delta^2 \|f\|^2, \quad (52)$$

where $\mathbf{h}^{(l)}(\mathcal{L})$ and $\mathbf{h}^{(l)}(\mathcal{L}')$ are manifold filters with filter function $h^{(l)}(\lambda)$ on the LB operators \mathcal{L} and \mathcal{L}' respectively. Combining the filter functions, we can write

$$\|\mathbf{h}(\mathcal{L})f - \mathbf{h}(\mathcal{L}')f\|^2 = \left\| \mathbf{h}^{(0)}(\mathcal{L})f + \sum_{l \in \mathcal{K}_m} \mathbf{h}^{(l)}(\mathcal{L})f - \mathbf{h}^{(0)}(\mathcal{L}')f - \sum_{l \in \mathcal{K}_m} \mathbf{h}^{(l)}(\mathcal{L}')f \right\|^2 \quad (53)$$

$$\leq \|\mathbf{h}^{(0)}(\mathcal{L})f - \mathbf{h}^{(0)}(\mathcal{L}')f\|^2 + \sum_{l \in \mathcal{K}_m} \|\mathbf{h}^{(l)}(\mathcal{L})f - \mathbf{h}^{(l)}(\mathcal{L}')f\|^2 \quad (54)$$

$$\leq \frac{(N_s + 1)\pi^2 \epsilon^2}{4(\alpha - \epsilon)^2} \|f\|^2 + A_h^2 \epsilon^2 \|f\|^2 + 4(N - N_s)\Delta^2 \|f\|^2. \quad (55)$$

We can extend the stability result to the MNN. To bound the output difference $\|\mathbf{y} - \mathbf{y}'\|$, we need to write in the form of features of the final layer

$$\|\mathbf{y} - \mathbf{y}'\|^2 = \sum_{q=1}^{F_L} \|f_L^q - f_L'^q\|^2. \quad (56)$$

The output signal of layer l of MNN $\Phi(\mathbf{H}, \mathcal{L}, f)$ can be written as

$$f_l^p = \sigma \left(\sum_{q=1}^{F_{l-1}} \mathbf{h}_l^{pq}(\mathcal{L}) f_{l-1}^q \right). \quad (57)$$

Similarly, for the perturbed \mathcal{L}' the corresponding MNN is $\Phi(\mathbf{H}, \mathcal{L}', f)$ the output signal can be written as

$$f_l'^p = \sigma \left(\sum_{q=1}^{F_{l-1}} \mathbf{h}_l^{pq}(\mathcal{L}') f_{l-1}^q \right). \quad (58)$$

The difference therefore becomes

$$\|f_l^p - f_l'^p\|^2 = \left\| \sigma \left(\sum_{q=1}^{F_{l-1}} \mathbf{h}_l^{pq}(\mathcal{L}) f_{l-1}^q \right) - \sigma \left(\sum_{q=1}^{F_{l-1}} \mathbf{h}_l^{pq}(\mathcal{L}') f_{l-1}^q \right) \right\|^2. \quad (59)$$

With the assumption that σ is normalized Lipschitz, we have

$$\|f_l^p - f_l'^p\|^2 \leq \left\| \sum_{q=1}^{F_{l-1}} \mathbf{h}_l^{pq}(\mathcal{L}) f_{l-1}^q - \mathbf{h}_l^{pq}(\mathcal{L}') f_{l-1}^q \right\|^2 \leq \sum_{q=1}^{F_{l-1}} \left\| \mathbf{h}_l^{pq}(\mathcal{L}) f_{l-1}^q - \mathbf{h}_l^{pq}(\mathcal{L}') f_{l-1}^q \right\|^2. \quad (60)$$

By adding and subtracting $\mathbf{h}_l^{pq}(\mathcal{L}') f_{l-1}^q$ from each term, combined with the triangle inequality we can get

$$\left\| \mathbf{h}_l^{pq}(\mathcal{L}) f_{l-1}^q - \mathbf{h}_l^{pq}(\mathcal{L}') f_{l-1}^q \right\|^2 \leq \left\| \mathbf{h}_l^{pq}(\mathcal{L}) f_{l-1}^q - \mathbf{h}_l^{pq}(\mathcal{L}') f_{l-1}^q \right\|^2 + \left\| \mathbf{h}_l^{pq}(\mathcal{L}') f_{l-1}^q - \mathbf{h}_l^{pq}(\mathcal{L}') f_{l-1}^q \right\|^2 \quad (61)$$

The first term can be bounded with (53) for absolute perturbations. The second term can be decomposed by Cauchy-Schwartz inequality and non-amplifying of the filter functions as

$$\left\| f_l^p - f_l'^p \right\|^2 \leq \sum_{q=1}^{F_{l-1}} C_{per} \epsilon^2 \|f_{l-1}^q\|^2 + \sum_{q=1}^{F_{l-1}} \|f_{l-1}^q - f_{l-1}^q\|^2, \quad (62)$$

where we use C_{per} to represent the terms in (53) for simplicity. To solve this recursion, we need to compute the bound for $\|f_l^p\|$. By normalized Lipschitz continuity of σ and the fact that $\sigma(0) = 0$, we can get

$$\|f_l^p\|^2 \leq \left\| \sum_{q=1}^{F_{l-1}} \mathbf{h}_l^{pq}(\mathcal{L}) f_{l-1}^q \right\|^2 \leq \sum_{q=1}^{F_{l-1}} \left\| \mathbf{h}_l^{pq}(\mathcal{L}) \right\|^2 \|f_{l-1}^q\|^2 \leq \sum_{q=1}^{F_{l-1}} \|f_{l-1}^q\|^2 \leq \prod_{l'=1}^{l-1} F_{l'} \sum_{q=1}^{F_0} \|f^q\|^2. \quad (63)$$

Insert this conclusion back to solve the recursion, we can get

$$\left\| f_l^p - f_l'^p \right\|^2 \leq l C_{per} \epsilon^2 \left(\prod_{l'=1}^{l-1} F_{l'} \right) \sum_{q=1}^{F_0} \|f^q\|^2. \quad (64)$$

Replace l with L we can obtain

$$\|\mathbf{y} - \mathbf{y}'\|^2 \leq \sum_{q=1}^{F_L} \left(L C_{per} \epsilon^2 \left(\prod_{l'=1}^{L-1} F_{l'} \right) \sum_{q=1}^{F_0} \|f^q\|^2 \right). \quad (65)$$

With $F_0 = F_L = 1$ and $F_l = F$ for $1 \leq l \leq L-1$, then we have

$$\|\mathbf{y} - \mathbf{y}'\|^2 \leq L F^{L-1} C_{per} \epsilon^2 \|f\|^2, \quad (66)$$

with $C_{per} = \frac{(N_s+1)\pi^2}{4(\alpha-\epsilon)^2} + A_h^2 + 4(N-N_s)\frac{\Delta^2}{\epsilon^2}$ as the terms in (53). \square

A.3 Proof of Theorem 4

The decomposition follows the same routine as (31) shows. By decomposing the filter function as (67) and (68), the norm difference can also be bounded separately.

$$h^{(0)}(\lambda) = \begin{cases} h(\lambda) - \sum_{l \in \mathcal{K}_m} h(C_l) & \lambda \in [\Lambda_k(\gamma)]_{k \in \mathcal{K}_s} \\ 0 & \text{otherwise} \end{cases} \quad \text{and} \quad (67)$$

$$h^{(l)}(\lambda) = \begin{cases} h(C_l) & \lambda \in [\Lambda_k(\gamma)]_{k \in \mathcal{K}_s} \\ h(\lambda) & \lambda \in \Lambda_l(\gamma) \\ 0 & \text{otherwise} \end{cases} \quad (68)$$

where now $h(\lambda) = h^{(0)}(\lambda) + \sum_{l \in \mathcal{K}_m} h^{(l)}(\lambda)$ with \mathcal{K}_s defined as the group index set of singletons and \mathcal{K}_m the set of partitions that contain multiple eigenvalues. For manifold filter $\mathbf{h}^{(0)}(\mathcal{L})$ with filter function $h^{(0)}(\lambda)$, the norm difference can also be written as

$$\begin{aligned} \left\| \sum_{i=1}^{\infty} h^{(0)}(\lambda_i) \langle f, \phi_i \rangle \phi_i - h^{(0)}(\lambda'_i) \langle f, \phi'_i \rangle \phi'_i \right\|^2 &\leq \sum_{i=1}^{\infty} |h^{(0)}(\lambda_i)|^2 \langle f, \phi_i \rangle^2 \|\phi_i - \phi'_i\|^2 \\ &+ \sum_{i=1}^{\infty} |h^{(0)}(\lambda_i)|^2 \langle f, \phi_i - \phi'_i \rangle^2 + \sum_{i=1}^{\infty} |h^{(0)}(\lambda_i) - h^{(0)}(\lambda'_i)|^2 \langle f, \phi'_i \rangle^2. \end{aligned} \quad (69)$$

Lemma 3. The eigenvalues of LB operators \mathcal{L} and perturbed $\mathcal{L}' = \mathcal{L} + \mathbf{E}\mathcal{L}$ with $\|\mathbf{E}\| = \epsilon$ satisfy

$$|\lambda_i - \lambda'_i| \leq \epsilon |\lambda_i|, \text{ for all } i = 1, 2 \dots \quad (70)$$

Proof of Lemma 3. With the assumption that $\mathcal{L}' = \mathcal{L} + \mathbf{E}\mathcal{L}$, we have

$$\lambda_i(\mathcal{L} + \mathbf{E}\mathcal{L}) = \max_{\text{codim } T \leq i-1} \min_{u \in T, \|u\|=1} \langle (\mathcal{L} + \mathbf{E}\mathcal{L})u, u \rangle \quad (71)$$

$$= \max_{\text{codim } T \leq i-1} \min_{u \in T, \|u\|=1} (\langle \mathcal{L}u, u \rangle + \langle \mathbf{E}\mathcal{L}u, u \rangle) \quad (72)$$

$$= \lambda_i(\mathcal{L}) + \max_{\text{codim } T \leq i-1} \min_{u \in T, \|u\|=1} \langle \mathbf{E}\mathcal{L}u, u \rangle. \quad (73)$$

For the second term, we have

$$|\langle \mathbf{E}\mathcal{L}u, u \rangle| \leq \langle |\mathbf{E}| |\mathcal{L}|u, u \rangle = \sum_n |\lambda_n(\mathbf{E})| |\lambda_n(\mathcal{L})| |\xi_n|^2 \quad (74)$$

$$\leq \max_n |\lambda_n(\mathbf{E})| \sum_n |\lambda_n(\mathcal{L})| |\xi_n|^2 = \|\mathbf{E}\| \langle |\mathcal{L}|u, u \rangle \leq \epsilon \langle |\mathcal{L}|u, u \rangle \quad (75)$$

Therefore, we have

$$\lambda_i(\mathcal{L} + \mathbf{E}\mathcal{L}) \leq \lambda_i(\mathcal{L}) + \epsilon \max_{\text{codim } T \leq i-1} \min_{u \in T, \|u\|=1} \langle |\mathcal{L}|u, u \rangle = \lambda_i(\mathcal{L}) + \epsilon |\lambda_i(\mathcal{L})|, \quad (76)$$

$$\lambda_i(\mathcal{L} + \mathbf{E}\mathcal{L}) \geq \lambda_i(\mathcal{L}) - \epsilon |\lambda_i(\mathcal{L})|, \quad (77)$$

$$\lambda_i(\mathcal{L}) - \epsilon |\lambda_i(\mathcal{L})| \leq \lambda_i(\mathcal{L} + \mathbf{E}\mathcal{L}) \leq \lambda_i(\mathcal{L}) + \epsilon |\lambda_i(\mathcal{L})|, \quad (78)$$

which concludes the proof. \square

The first two terms of (69) rely on the differences of eigenfunctions, which can be derived with Davis-Kahan Theorem in Lemma 2, the difference of eigenfunctions can be written as

$$\|\mathbf{E}\mathcal{L}\phi_i\| = \|\mathbf{E}\lambda_i\phi_i\| = \lambda_i \|\mathbf{E}\phi_i\| \leq \lambda_i \|\mathbf{E}\| \|\phi_i\| \leq \lambda_i \epsilon. \quad (79)$$

The first term in (69) then can be bounded as

$$\sum_{i=1}^{\infty} |h^{(0)}(\lambda_i)|^2 \langle f, \phi_i \rangle^2 \|\phi_i - \phi'_i\|^2 \leq \sum_{i=1}^{\infty} \langle f, \phi_i \rangle^2 \left(\frac{\pi \lambda_i \epsilon}{d_i} \right)^2. \quad (80)$$

Because $d_i = \min\{|\lambda_i - \lambda'_{i-1}|, |\lambda'_i - \lambda_{i-1}|, |\lambda'_{i+1} - \lambda_i|, |\lambda_{i+1} - \lambda'_i|\}$, with Lemma 3 implied, we have

$$|\lambda_i - \lambda'_{i-1}| \geq |\lambda_i - (1 + \epsilon)\lambda_{i-1}|, |\lambda'_i - \lambda_{i-1}| \geq |(1 - \epsilon)\lambda_i - \lambda_{i-1}|, \quad (81)$$

$$|\lambda'_{i+1} - \lambda_i| \geq |(1 - \epsilon)\lambda_{i+1} - \lambda_i|, |\lambda_{i+1} - \lambda'_i| \geq |\lambda_{i+1} - (1 + \epsilon)\lambda_i|. \quad (82)$$

Combine with Lemma 3 and Definition 6, $d_i \geq \epsilon\gamma + \gamma - \epsilon$:

$$|(1 - \epsilon)\lambda_{i+1} - \lambda_i| \geq |\gamma\lambda_i - \epsilon\lambda_{i+1}| = \epsilon\lambda_i \left| 1 - \frac{\lambda_{i+1}}{\lambda_n} + \frac{\gamma}{\epsilon} - 1 \right| \geq \lambda_i(\gamma - \epsilon + \gamma\epsilon) \quad (83)$$

This leads to the bound as

$$\sum_{i=1}^{\infty} |h^{(0)}(\lambda_i)|^2 \langle f, \phi_i \rangle^2 \|\phi_i - \phi'_i\|^2 \leq \left(\frac{\pi\epsilon}{\gamma - \epsilon + \gamma\epsilon} \right)^2 \|f\|^2. \quad (84)$$

The second term in (69) can be bounded as

$$\sum_{i=1}^{\infty} |h^{(0)}(\lambda_i)|^2 \langle f, \phi_i - \phi'_i \rangle^2 \leq M_s \left(\frac{\pi\epsilon}{\gamma - \epsilon + \gamma\epsilon} \right)^2 \|f\|^2, \quad (85)$$

which similarly results from the fact that $|h^{(0)}(\lambda)| < 1$ and $h^{(0)}(\lambda) = 0$ for $\lambda \in [\Lambda_k(\gamma)]_{k \in \mathcal{K}_m}$. The number of eigenvalues within $[\Lambda_k(\gamma)]_{k \in \mathcal{K}_s}$ is denoted as M_s .

The third term in (69) is:

$$\sum_{i=1}^{\infty} |h^{(0)}(\lambda_i) - h^{(0)}(\lambda'_i)|^2 \langle f, \phi'_i \rangle^2 \leq \left(\frac{B_h\epsilon|\lambda_i|}{(\lambda_i + \lambda'_i)/2} \right)^2 \sum_{i=1}^{\infty} \langle f, \phi'_i \rangle^2 \leq \left(\frac{2B_h\epsilon}{2 - \epsilon} \right)^2 \|f\|^2, \quad (86)$$

with the use of Lemma 3 and Definition 8.

Then we need to analyze the output difference of $h^{(l)}(\lambda)$.

$$\left\| \mathbf{h}^{(l)}(\mathcal{L})f - \mathbf{h}^{(l)}(\mathcal{L}')f \right\|^2 \leq \|(h(C_l) + \Delta)f - (h(C_l) - \Delta)f\|^2 \leq 4\Delta^2\|f\|^2. \quad (87)$$

Combine the filter function, we could get

$$\|\mathbf{h}(\mathcal{L})f - \mathbf{h}(\mathcal{L}')f\|^2 = \|\mathbf{h}^{(0)}(\mathcal{L})f + \sum_{l \in \mathcal{K}_m} \mathbf{h}^{(l)}(\mathcal{L})f - \mathbf{h}^{(0)}(\mathcal{L}')f - \sum_{l \in \mathcal{K}_m} \mathbf{h}^{(l)}(\mathcal{L}')f\|^2 \quad (88)$$

$$\leq \|\mathbf{h}^{(0)}(\mathcal{L})f - \mathbf{h}^{(0)}(\mathcal{L}')f\| + \sum_{l \in \mathcal{K}_m} \|\mathbf{h}^{(l)}(\mathcal{L})f - \mathbf{h}^{(l)}(\mathcal{L}')f\|^2 \quad (89)$$

$$\leq \frac{(M_s + 1)\pi^2\epsilon^2}{(\gamma - \epsilon + \gamma\epsilon)^2} \|f\|^2 + \left(\frac{2B_h\epsilon}{2 - \epsilon} \right)^2 \|f\|^2 + 4(M - M_s)\Delta^2\|f\|^2. \quad (90)$$

For the stability of MNN with γ -FRT filters, the result can be derived with the same routine but replace the C_{per} term as $C_{per} = \frac{(M_s + 1)\pi^2}{(\gamma - \epsilon + \gamma\epsilon)^2} + \left(\frac{2B_h}{2 - \epsilon} \right)^2 + \frac{4(M - M_s)\Delta^2}{\epsilon^2}$.

A.4 Proof of Theorem 1

Theorem 2 shows that the manifold deformation $v(x) = x + \tau(x)$ with $\|\tau(x)\| = \epsilon$ and $\|\nabla\tau(x)\| = \epsilon$ can be seen as perturbations to the Laplace-Beltrami operator $\mathcal{L} - \mathcal{L}' = \mathbf{E}\mathcal{L} + \mathbf{A}$ with $\|\mathbf{E}\| = \epsilon$ and $\|\mathbf{A}\| = \epsilon$. This is a combination of Theorem 3 and Theorem 4. By setting the γ -FRT filter with $\gamma = \alpha/\lambda_1$, eigenvalues $\lambda_i, \lambda_{i+1} \in \Lambda_k(\gamma)$ would lead to $\lambda_i, \lambda_{i+1} \in \Lambda_l(\alpha)$ due to the fact that

$$\lambda_{i+1} - \lambda_i \leq \gamma\lambda_i = \frac{\alpha}{\lambda_1}\lambda_i \leq \alpha. \quad (91)$$

We can state our main theorem more formally as follows

Theorem 5. Let \mathcal{M} be a manifold with LB operator \mathcal{L} and f be manifold data. We construct $\Phi(\mathbf{H}, \mathcal{L}, f)$ as a MNN on \mathcal{M} (10) where the filters $\mathbf{h}(\mathcal{L})$ are α -FDT [cf. Definition 3], α/λ_1 -FRT [cf. Definition 7], A_h -Lipschitz [cf. Definition 4] and B_h -integral Lipschitz [cf. Definition 8]. Consider a deformation on \mathcal{M} as $v(x) = x + \tau(x) \in \mathcal{M}$ where $\|\tau(x)\| = \epsilon$ and $\|\nabla\tau(x)\| = \epsilon$ with $\epsilon \ll \min(\alpha/\lambda_1, \alpha, 2)$. Then under Assumptions 2 and 3 it holds that

$$\Phi(\mathbf{H}, \mathcal{L}, f) - \Phi(\mathbf{H}, \mathcal{L}', f) = O(\epsilon^2)\|f\|^2. \quad (92)$$

A.5 Simulations

We train the GNNs with tensorflow in Python. We use the Adam gradient descent method with the learning rate set as 0.003. The channel conditions of all links can be represented by a matrix $\mathbf{S}(t)$ with each element $[\mathbf{S}(t)]_{ij} := s_{ij}(t)$ denotes the channel condition between transmitter i and receiver $r(j)$. We construct the channel condition by considering the large-scale path-loss gain and a random fast fading gain, which can be written as: $s_{ij} = d_{ij}^{-2.2} s^f$, where d_{ij} stands for the distance between transmitter i and receiver $r(j)$, while $s^f \sim \text{Rayleigh}(2)$ is the random fading.